Cell Biochem Biophys (2018) 76:173–185
DOI 10.1007/s12013-017-0818-1

ORIGINAL PAPER

Identification and characterization of functional single nucleotide polymorphisms (SNPs) in Axin 1 gene: a molecular dynamics approach

Imran Khan[1] · Irfan A. Ansari[1] · Pratichi Singh[2] · J. Febin Prabhu Dass[2] · Fahad Khan[1]

Received: 16 October 2016 / Accepted: 19 July 2017 / Published online: 2 August 2017

Abstract Wnt signaling pathway has been reported to play crucial role in intestinal crypt formation and deregulation of this pathway is responsible for colorectal cancer initiation and progression. Axin 1, a scaffold protein, play pivotal role in the regulation of Wnt/β-catenin signaling pathway and has been found to be mutated in several cancers; primarily in colon cancer. Considering its crucial role, a structural and functional analysis of missense mutations in Axin 1 gene was performed in this study. Initially, one hundred non-synonymous single nucleotide polymorphisms in the coding regions of Axin 1 gene were selected for in silico analysis. Six variants (G820S, G856S, E830K, L811V, L847V, and R767C) were predicted to be deleterious by combinatorial prediction. Further investigation of structural attributes confirmed two highly deleterious single nucleotide polymorphisms (G820S and G856S). Molecular dynamics simulation demonstrated variation in different structural attributes between native and two highly deleterious Axin 1 mutant models. Finally, docking analysis showed variation in binding affinity of mutant Axin 1 proteins with two destruction complex members, GSK3β and adenomatous polyposis. The results collectively showed the deleterious effect of the above predicted single nucleotide polymorphisms on the Axin 1 protein structure and could prove to be an adjunct in the disease genotype-phenotype correlation studies.

Keywords Colorectal cancer · Axin 1 · molecular dynamics · SNPs and molecular docking

✉ Irfan A. Ansari
iaansari@iul.ac.in

[1] Department of Biosciences, Integral University, Lucknow, India

[2] School of Biosciences and Technology, Vellore Institute of Technology, Vellore, Tamilnadu, India

Introduction

Globally colorectal cancer (CRC) has been reported as one of the major cause of increasing morbidity and mortality. Most well documented pathway associated with the pathophysiology of CRC is Wnt pathway [1]. Wnt pathway is implicated in intestinal crypt cell proliferation and homeostasis [2, 3]. This pathway is activated via binding of Wnt ligands to the transmembrane frizzled (Fz or Fzd) receptors or to low density lipoprotein receptor-related proteins (LRP6and LRP7), its co-receptor proteins;causing the inhibition of the destruction complex and transport of β-catenin into the nucleus. Finally, this event leads to activation of Wnt target genes. In the absence of Wnt ligands, the destruction complex, composed of scaffolding protein Axin, casein kinase (CK1), adenomatous polyposis (APC), and glycogen synthase kinase 3 (GSK3), constantly degrades the cytoplasmic β-catenin protein. This prevents β-catenin from entering the nucleus and represses the Wnt target genes [4]. Axin was initially identified as the gene product of the mouse fused locus, which negatively regulates Wnt signaling [5]. Axin possess multiple domains having binding capacity for GSK-3β, APC, β-catenin, disheveled, protein phosphatase 2 A, and Axin itself [6, 7]. Axin, being a scaffold protein in this multiprotein complex, brings β-catenin and GSK-3 β into close proximity, thereby, facilitating the phospholrylation of β-catenin and consequently, activating ubiquitin-mediated degradation by proteasome system [8–10]. Recent studies have suggested that Axin forms a dimer for its inhibitory function in TCF/LEF1 transcription [11–13]. Alterations in the Wnt pathway is reported to contribute to the pathogenesis of CRC [14–17]. In particular, the most documented mutations, associated with CRC pertaining Wnt pathway, is in APC gene [18]. Other important component of Wnt pathways mutated in several cancers is Axin1 gene [19].

Recent advances in in silico methods have provided an efficient method for identification of non-synonymous/missense single nucleotide polymorphism (nsSNPs) within the protein coding regions of a gene, implementing structural attributes and sequence based information. These computational programs classify these single nucleotide polymorphisms (SNPs) as deleterious and non-deleterious through considering various aspects like physiochemical properties, sequence conservation among various species and structural features of a protein [20–24]. Structural variation in protein resulting from amino acid substitution depends on the location of the substitution in protein sequence and the biochemical properties like acidic, basic or hydrophobic nature of protein [25]. So, recognizing the importance of down-stream regulatory scaffold protein for destruction complex (Axin1), we employed support vector based approaches and empirical based methods to profile deleterious nsSNPs of Axin1 gene. Thus, the goal of the present study was to identify deleterious nsSNPs in Axin1 gene which could alter the functional and structural aspects of Axin1 protein.

Materials and Methods

SNP Data Retrival

The SNPs were retrieved from SNP database of National Center for Biotechnology Information (NCBI) (http://www.ncbi.nlm.nih.gov/snp) through encorpotating various limits of *Homo sapiens*, stop gained, coding synonymous, coding non-synonymous, mRNA UTR (5′ and 3′) and intronic regions [26].

Sequence based Evaluation of Coding Single Nucleotide Polymorphism

PROVEAN (Protein Variation Effect Analyzer), found at http://provean.jcvi.org, is a sequence based bioinformatics tool which predicts functional effects of multiple amino acid substitution, deletions and insertions on protein's biological function. The tool analyzes the SNPs at default threshold value of 0.1. If the PROVEAN score is smaller than or equal to a given threshold, the variation is predicted as deleterious [27].

Structure based Evaluation of Coding Single Nucleotide Polymorphism

PolyPhen-2 (Polymorphism Phenotyping v2), (http://genetics.bwh.harvard.edu/pph2/), is an automated structural homology based tool that predicts the impact of amino acid substitution on the protein [28, 29]. A position-specific independent counts (PSIC) score and their difference is generated for two variants. The PSIC score of 1.5 or above is characterized as damaging. The PolyPhen PSIC scores are classified as probably damaging (2.00), possibly damaging (1.50–1.99), potentially damaging (1.25–1.49), or benign (0.00–0.99). I-Mutant 2.0 (http://folding.uib.es/cgi-bin/i-mutant2.0.cgi) is classified under support vector machine (SVM)-based web server for predicting the protein stability changes upon single point mutations. This tool predicts the free energy change (ΔΔG) calculated through subtracting the free energy changes between the mutant and native protein structures (Kcal/mol) [30]. Zero value of ΔΔG represented high stability and more negative values denoted the lower stability of mutant protein.

3D-Structure Modeling

Structural stability of the protein upon substitution was analyzed through X-ray crystallographic 3-D structure of Axin1 protein (pdb id-1DK8, 4B7T, and 2D5G), downloaded from the UniProt (pdb usm). These structures were further validated from PROCHECK (http://www.ebi.ac.uk/thornton-srv/software/PROCHECK/) [31, 32]. SWISS PDB Viewer was used to generate mutant protein models. To bring the protein models to its most favorable conformation energy minimization is required, Energy minimizations for the native and the mutant structures performed by NOMAD-Ref (http://lorentz.immstr.pasteur.fr/nomad-ref.php) which uses Gromacs algorithm by default [33].

Investigation of Structural Attributes

SPPIDER (Solvent accessibility based Protein-Protein Interface iDEntification and Recognition) (http://sppider.cchmc.org/) is a server that predicts the solvent accessibility and secondary structures in the 3D structure of proteins [34]. The server used Polyview3D–Dictionary of Secondary Structure Protein (DSSP) for the prediction of secondary structure and solvent accessibilities (SABLE) for solvent accessibility. SRide (http://sride.enzim.hu/) server was used for the screening of stabilizing residues (SRs) which play significant role in protein 3D-stucture stabilization. High conservation of these stabilizing residues is reported among protein sequences [35]. FlexPred (http://flexpred.rit.albany.edu/) web-server was used for predicting residue positions involved in conformational switches in proteins. This web-server predicts residue positions that may be involved in such ordered conformational switches. The output from FlexPred consists of labels 'R' (rigid) and 'F' (flexible) [36]. HBAT is a freely available tool for the automated analysis of protein structure PDB files for all non-bonded interactions [37].

Molecular Dynamics Simulation Protocol

GROMACS 4.5.3 program package with GROMOS9643a1 force field for energy minimization was employed for the molecular dynamics simulation studies [38]. Furthermore, the trajectory files for mutant and native models of Axin1 protein were generated by built in functions of GROMACS 4.5.3. Trajectory files were analyzed using g_rms, g_rmsf, g_sas GROMACS utilities for total energy, root mean square deviation (RMSD), root mean square fluctuation (RMSF) and solvent accessibility surface area (SASA). The g_hbond function was used to calculate the number of various hydrogen bonds formed in the protein during simulation. The number of hydrogen bonds were determined at donor-hydrogen-acceptor angle larger than 90° and donor-acceptor distance less than 3.5 A° (0.35 nm) We have confirmed that our systems were equilibrated for 1 nanosecond (ns) under the NPT ensemble (constant temperature: 300 K and pressure: 1 atm) conditions [39].

Molecular Docking Analysis

The docking analysis of native and mutant Axin1 proteins with two destruction complex proteins (GSK3β and APC) was performed by HEX 5.1 docking software [40]. Hex is an Interactive Molecular Graphics Program that calculates and displays possible docking modes of pair of proteins. The parameters opted for the analysis were;(1) Correlation type-Shape + Electrostatics, (2) FFT Mode–3D, (3) Post Processing–MM Energies, (4) Grid Dimension–0.6, (5) Receptor Range–180, (6) Ligand Range–180, (7) Twist Range–360 and Distance Range−40. 3D structures for GSK3β and APC were downloaded from uniprot having PDB ids-3DU8 and 3NMZ, respectively. The flow chart of methodology is shown in Fig. 1.

Furthermore, docking analysis was validated by incorporating ZDOCK server. ZDOCK is a rigid-body protein-protein docking server. It utilizes Fast Fourier Transform algorithm for an efficient global docking on the 3D grid. It also utilizes the combination of electrostatic, shape complementarity and statistical potential for scoring the docked complex [41].

Results

Data Mining

For the present study, we selected SNPs of Axin1 gene for *Homo sapiens* through encorpotating various limits of stop gained, coding synonymous, coding non-synonymous, mRNA UTR (5' and 3') and intronic regions. Out of 1898 SNPs, coding region contains 100 nsSNPs (5.25%) and

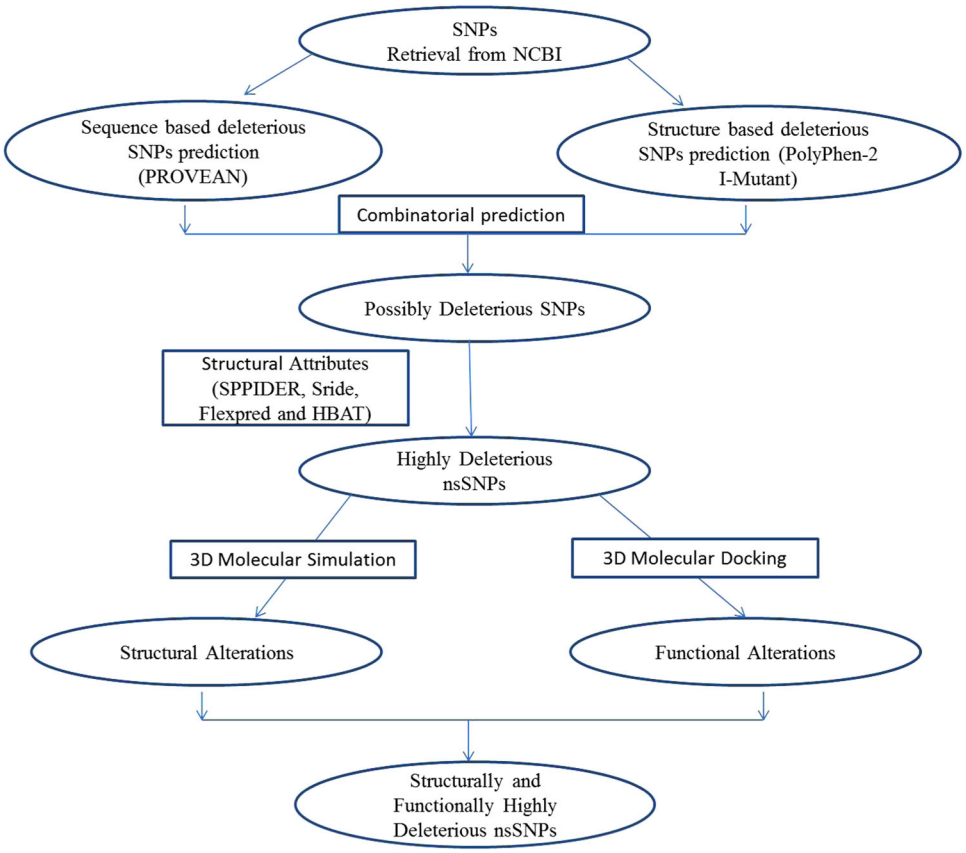

Fig. 1 Schematic overview of methodology

73 sSNPs (3.83%) and non-coding regions contain 1689 SNPs (88.80%) in intronic regions and 36 SNPs (1.88%) in mRNA UTR region with 5 SNPs in 5′ UTR and 31 SNPs in 3′ UTR. Since, majority of SNPs were found to be in intronic region, therefore, SNPs found within regulatory region or coding non-synonymous region (100 nsSNPs) of Axin1 gene were selected for our investigation. Various bioinformatics tools were further implemented to assess the functional impact of these sorted nsSNPs shown in Fig. 2.

Sequence Based Evaluation of Coding Single Nucleotide Polymorphism

Out of 100 nsSNPs, 32 nsSNPs (32%) were predicted to be deleterious with ≤ 2.5 scores. On the other side 68 nsSNPs (68%) showed the score > 2.5 and were denoted as neutral. Thus, total 32 nsSNPs (32%) were predicted to be deleterious that may alter functional properties of protein. Therefore, these scores enable the quantitative comparison and ranking the nsSNPs according to their deleterious nature and allow researchers to decide those SNPs to be targeted for further investigation.

Analysis of Deleterious nsSNPs Using PolyPhen-2

Out of 100 nSNPs, 19 nsSNPs (19%) were found to be probably damaging depicting PSIC score values ranging from 0.8 to 1; 33 nsSNPs (33%) were predicted to be possibly damaging having score values 0.6–0.8; and 48 nsSNPs (48%) were categorized as benign (neutral) with score value zero. Thus PolyPhen scores are convenient in quantitatively characterizing the the damaging effect of nsSNPs on protein function.

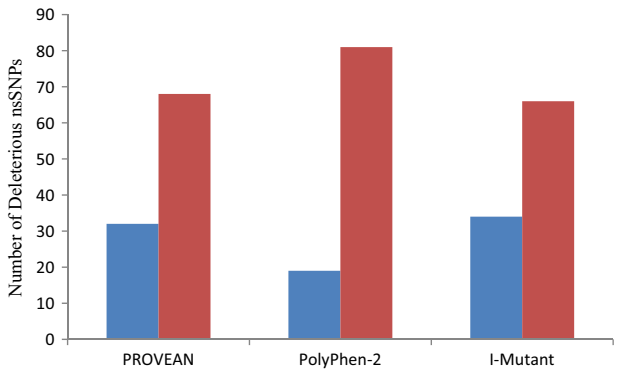

Fig. 2 Prediction of deleterious nsSNPs in AXIN 1 gene by SIFT, Polyphen-2, and I-Mutant 2.0. The bar diagram depicts the number of deleterious and benign nsSNPs predicted by all three tools, the *red bar* indicates the benign nsSNPs and *blue bar* denotes the deleterious nsSNPs (color figure online)

Analysis of Deleterious nsSNPs Using I-MUTANT 2.0

According to I-Mutant 2.0, more negative the values of free energy change (DDG), lesser will be the stability of protein. According to these scores, out of 100 nsSNPs, 34 variants showed DDG values ranging from -1.0 to -4.21 which were considered to be least stable and most deleterious nsSNPs. The other 35 variants, having DDG values ranging from -0.01 to -0.99, were further categorized as less stable and mildly deleterious nsSNPs. The remaining 31 variants showed DDG values ranging from 0.01 to 1.03 which were identified as non-deleterious. Thus, total 69 nsSNPs/variants (69%) were predicted by I-Mutant 2.0 to be deleterious to the protein stability.

Combinatorial Prediction of Functionally Deleterious nsSNPs

Since all the tools work on a specific algorithm which rely on variable biological aspects; thus, by combining various different computational tools, prediction of highly deleterious nsSNPs can be performed with greater accuracy [42, 43]. Thus in order to minimize the false positive predictions, we employed combinatorial approach encorporating both support vector machine (SVM) and empirical based tools and selected only those SNPs for further structural analysis which were commonly predicted to be deleterious by all tools. By comparing the results of PROVEAN, PolyPhen-2, and I-Mutant 2.0 tools, 6 variants G820S, G856S, E830K, L811V, L847V, and R767C having SNP IDs rs142888154, rs142888154, rs142888154, rs149865527, rs149865527, and rs151104297 respectively, were predicted to be functionally deleterious by all four tools. Table 1 displays the predicted scores of PROVEAN, PolyPhen 2.0 and I-Mutant 2.0. These 6 nsSNPs were selected for further trajectory analysis.

Modeling of Mutant Protein Structures

SNPs can significantly alter the protein stability. Thus, to gain better insight in to single nucleotide change and its role in structural and functional stability of protein, it is obligatory to gather knowledge about 3D structure. The multiple 3D structures of Axin1 protein, to complete the trajectory analysis, were obtained from Universal Protein Resource (UniProt), followed by the validation of the native structure by using PROCHECK server. The structure had resolution of 1.57, 2.40, and 2.90 A° and Ramachandran plot depicted the presence of higher number of residues in most favored region. Mutant models for the 6 nsSNPs, sorted via combinatorial analysis, were generated using SWISSPDB Viewer. For further analysis, three-dimensional structures were energy minimized using NOMAD-Ref

server. Thus, 6 nsSNPs (G820S, G856S, E830K, L811V, L847V, and R767C) were referred to as highly deleterious nsSNPs for the 3D-protein structures and further trajectory analysis was performed to investigate accurately the deleterious effect of these highly deleterious nsSNPs on the 3D Axin1 protein structure and function.

Structural Investigation

SPPIDER server predicted G820S, G856S, and L847V nsSNP with variation in the solvent accessibilities from buried to exposed, thus increasing the solvent accessibility of the mutant models (Table 2). Further, the analysis of stabilizing residues in all the 6 mutant models by SRide server predicted variation in the stabilizing residues of G820S and G856S, shown in Table 3. Thus, comparing these results and applying the combinatorial approach to remove false positive results,we selected G820S and G856S mutant models for further investigation of structural attributes since, these two G > S mutations were flagged by SPPIDER and SRide, whereas the L847V mutant was flagged only in SPPIDER. The flexpred server predicted the variation in the flexible residues in both mutant (G820S and G856S) and native Axin1 protein model, shown in Table 4. Mutant models G820S and G856S showed the addition of flexible residues at same positions of 13, 15, 55, 86, 97, 100, 124, 125, 134, 135, 136, 138, 139, 169, 170, 171, 172, 208, 209, 223, 224, and 225. Similarly, positions of deletion in flexible residues were also predicted to be same in both the mutant models by flexpred (96, 133, 206, 207, 217, and 218).

Furthermore, a countable change in hydrogen bond frequencies was noticed in both the highly deleterious nsSNP G820S and G856S models compared to native protein structure shown in Table 5. Both the selected highly deleterious nsSNPs showed variation in the strong and weak H-bonds. A notable decrease in the strong H-bond N–H..O and increase in weak H- bonds like C–H..O and C–H..N was predicted by HBAT tool. The investigation reveals that these nsSNPs were the most possible highly deleterious and may affect the 3D-structure of the Axin1 protein.

Molecular Dynamics Simulation

To further gain better understanding of the conformational changes of the 3D structures, molecular dynamics simulation of both the mutant (G820S and G856S) models and native Axin1 protein was performed for the time period of 100 nanoseconds (ns). The trajectory files were generated and analyzed for RMSD, RMSF, radius of gyration (Rg), hydrogen bond and solvent accessible surface (SAS).

We analyzed the RMSD value for the Cα atom of native and mutant models shown in Fig. 3. The realtime variation of RMSD values of native model showed fluctuation from ~0.1 to ~0.4 nm. Mutant model G820S showed fluctuation ranging from ~0.8 to ~0.32 nm. On the other side, mutant

Table 1 Combined prediction of PROVEAN, PolyPhen 2.0, I-Mutant 2.0 and PANTHER for possible deleterious nsSNPs of Axin-1 gene

Sl. No.	rsID	Allele	Position	Residue change	PROVEAN prediction	PolyPhen-2 Score	I-Mutant DDG
1	rs142888154	G/A	G820S	G [Gly] ⇒ S [Ser]	−4.514	0.997	−0.9
2	rs142888154	G/A	G856S	G [Gly] ⇒ S [Ser]	−4.316	1.000	−3.04
3	rs142888154	G/A	E830K	E [Glu] ⇒ K [Lys]	−3.357	0.945	−3.43
4	rs149865527	C/G	L811V	L [Leu] ⇒ V [Val]	−2.57	0.999	−1.38
5	rs149865527	C/G	L847V	L [Leu] ⇒ V [Val]	−2.549	0.999	−0.91
6	rs151104297	C/T	R767C	R [Arg] ⇒ C [Cys]	−4.622	0.915	−2.21

Table 2 Comparative analysis of solvent accessibility (SABLE) and secondary structures of native and mutant Axin-1 protein predicted by SPPIDER

			Secondary structure		Solvent accessibility–SABLE	
Sl. No.	Position	rsID	Native	Mutant	Native	Mutant
1	G820S	rs142888154	E	E	**FULLY BURRIED**	**FULLY EXPOSED**
2	G856S	rs142888154	E	E	**FULLY BURRIED**	**FULLY EXPOSED**
3	E830K	rs142888154	C	C	SLIGHTLY EXPOSED (4)	SLIGHTLY EXPOSED (5)
4	L811V	rs149865527	E	E	FULLY BURRIED	FULLY BURRIED
5	L847V	rs149865527	E	E	**FULLY BURRIED**	**SLIGHTLY EXPOSED (2)**
6	R767C	rs151104297	C	C	SLIGHTLY EXPOSED (5)	SLIGHTLY EXPOSED (4)

Note: *C* Coil, *E* beta Strand, [9-Fully Exposed; 0 – Fully Buried]

Table 3 Stabilizing residues of native and mutant Axin-1 proteins analyzed by SRide

Sl. No.	Substitutions	Stablizing residues	
		Existing	Newly formed
1	Native		
2	G [Gly] ⇒ S [Ser]	VAL749,TYR751,PHE788, LYS789, GLY820,VAL822	VAL749,TYR751,PHE788, LYS789, **SER820**, -, VAL822
3	G [Gly] ⇒ S [Ser]	VAL785,TYR787,PHE824, LYS825, GLY856,VAL858	VAL785,TYR787,PHE824, LYS825, **SER856**, -, VAL858
4	E [Glu] ⇒ K [Lys]	VAL785,TYR787,PHE824, LYS825, GLY856,VAL858	VAL785,TYR787,PHE824, LYS825, GLY856,VAL858
5	L [Leu] ⇒ V [Val]	VAL749,TYR751,PHE788, LYS789, GLY820,VAL822	VAL749,TYR751,PHE788, LYS789, GLY820,VAL822
6	L [Leu] ⇒ V [Val]	VAL785,TYR787,PHE824, LYS825, GLY856,VAL858	VAL785,TYR787,PHE824, LYS825, GLY856,VAL858

Note: (-) indicates deletion of particular stabilizing residues in mutant models that existed in native protein model and residues in bold denotes newly formed SR

Table 4 Variations in flexible residue positions in native and mutant Axin-1 protein structures

Sl. No.	Residue change	Rs ID	Flexible residues
1	Native		12, 14, 37, 38, 39, 40, 49, 50, 51, 52, 53, 54, 83, 85, 96, 98, 99, 121, 122, 123, 133, 206, 207, 217, 218, 219, 220, 221, 222,
2	G [Gly] ⇒ S [Ser]	rs142888154	12, **13**, 14, **15**, 37, 38, 39, 40, 49, 50, 51, 52, 53, 54, **55**, 83, 84, 85**, 86**,-, **97**, 98, 99, **100**, 122, 123, **124, 125**,-, **134, 135, 136, 138, 139, 169, 170, 171, 172**, -, -, **208, 209**,-, -, 219, 220, 221, 222, **223, 224, 225**
3	G [Gly] ⇒ S [Ser]	rs142888154	12, **13**, 14, **15**, 37, 38, 39, 40, 49, 50, 51, 52, 53, 54, **55**, 83, 84, 85**, 86**,-, **97**, 98, 99, **100**, 122, 123, **124, 125**,-, **134, 135, 136, 138, 139, 169, 170, 171, 172**, -, -, **208, 209**,-, -, 219, 220, 221, 222, **223, 224, 225**

Note: (-) indicates deletion of particular flexible residues in mutant models that existed in native protein model and residues in bold denotes newly formed flexible residues in mutant models

Table 5 Intermolecular hydrogen bond frequency predictions in native and mutant Axin-1 proteins by HBAT

Sl. No.	Residue change	rs ID	N–H..O	O–H..O	N–H..N	O–H..N	C–H..O	C–H..N	N–H..S	O–H..S	C–H..S
1	Native		**244**	14	71	6	**72**	**8**	5	0	5
2	G [Gly] ⇒ S [Ser]	rs142888154	**248**	14	71	6	**75**	**10**	5	0	5
3	G [Gly] ⇒ S [Ser]	rs142888154	**248**	14	71	6	**75**	**10**	5	0	5

model G856S showed greater fluctuation ranging from ~0.14 to ~0.25 nm. During the early ~25 ns of MD simulation mutant model G856S and G820S followed similar pattern of fluctuation as of native model. After this, an abrupt decrease in RMSD value of mutant model G856S and G820S was observed after ~30 ns of MD simulation ranging from ~0.15 to ~0.25 nm and ~0.12 to ~0.32 compared to compare to native Axin1 protein having values ranging from ~0.25 to ~0.32. This magnitude of fluctuation along with minor differences in average RMSD values after relaxation period (~0.25 nm) depicted the stable simulation trajectory. This deviation of RMSD values of mutant models from the native model depicts the possible deleterious effect of these single nucleotide polymorphisms causing the changes in stability. To determine the effect of mutations in the dynamic behavior of residues, RMSF values of the mutant and native Axin1 models were analyzed. The native model showed RMSF values ranging from ~0.1 to ~0.7, depicting a higher degree of flexibility in the backbone residues. On the other hand the mutant models showed significantly lower level of backbone residue flexibility. Generally, glycine is highly flexible in nature and most predominantly located in turns, facilitating proper 3D-folding to keep protein functionally active. In our study glycine residues were located at 820 and 856 positions, and their substitution by serine residues would definitely have

significant impact on folding conformations of protein. Mutant G820S model depicted comparatively lower residue flexibility with highest RMSF values of ~0.2 nm. Whereas, mutant G856S model showed slightly higher flexibility having RMSF values to highest of ~0.38 nm.

To understand the variations in the atomic distribution in the mutant and native Axin1 models, Rg values were also analyzed (Fig. 3). Significant decrease in the Rg values of mutant model G856S and G820S was observed throughout the simulation. The realtime variation of Rg values of native model showed fluctuation from ~1.5 to ~1.65 nm. Mutant model G820S showed fluctuation ranging from ~1.55 to ~1.6 nm. On the other side mutant model G856S showed higher decrease in the Rg values over the simulation

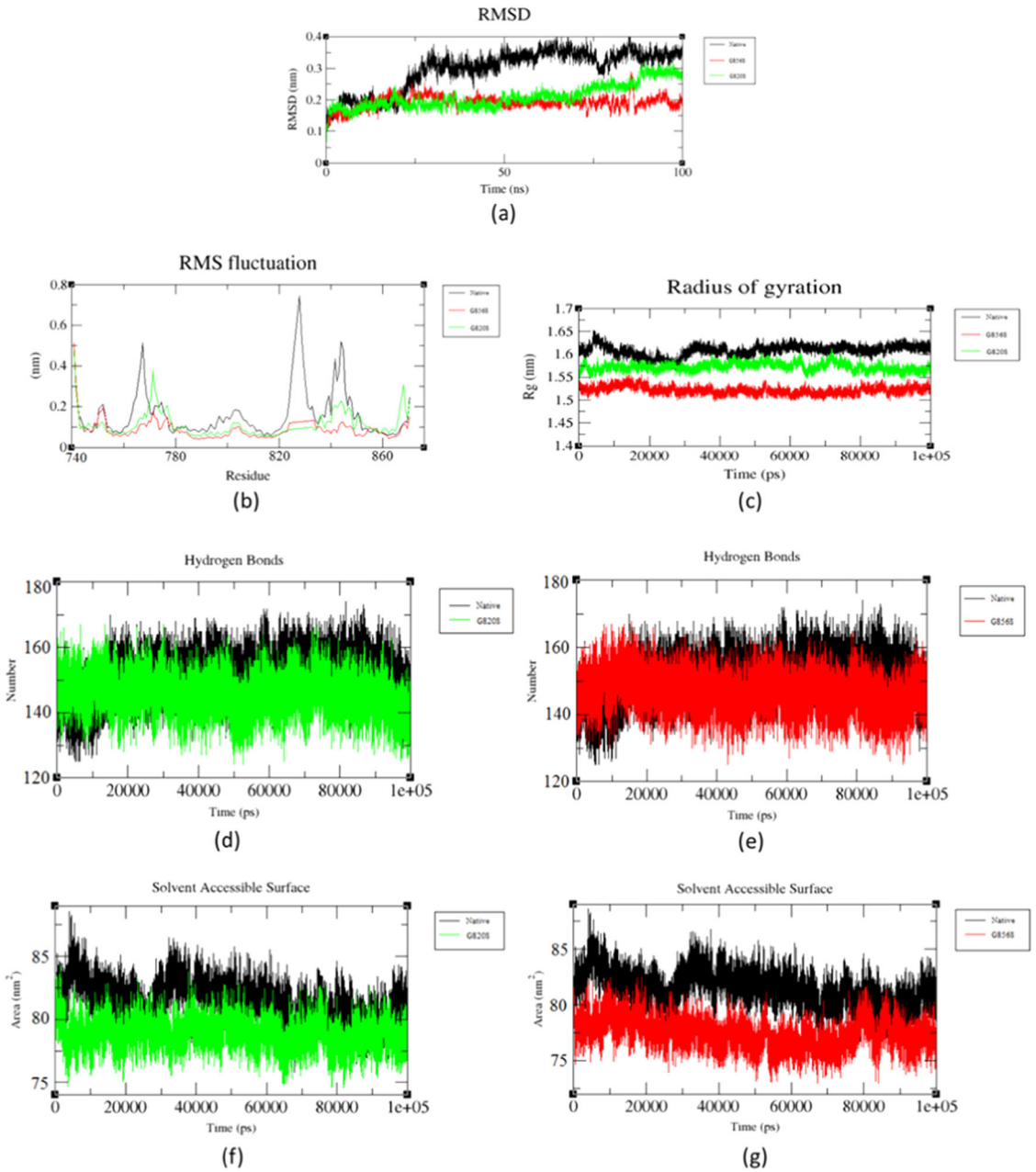

Fig. 3 MD trajectory file analysis **a** Backbone RMSD values of the native and mutant AXIN1 protein. The ordinate is RMSD (nm), and the abscissa is time (ps). **b** RMSF value of the native and mutant AXIN1 protein. **c** Rg of the backbone carbon alpha for the native and mutant AXIN1 protein. The ordinate is Rg (nm), and the abscissa is time (ps). **d** Number of hydrogen bonds formed in native and mutant G820S AXIN1 protein. **e** Number of hydrogen bonds formed in native and mutant G856S AXIN1 protein. The ordinate is RMSD (nm), and the abscissa is time (ps). **f** Solvent accessible surface area of the native and mutant G820S AXIN1 protein. **g** Solvent accessible surface area of the native and mutant G856S AXIN1 protein. The ordinate is Area (nm^2), and the abscissa is time (ps). The green, red and black lines indicate the native, G820S and G856S structures, respectively

ranging from ~1.5 to ~1.55 nm. The results depict the less expanded conformation of mutant Axin1 protein, thus directing towards the variation in the conformational changes in the Axin1 protein possibly caused by the single nucleotide polymorphisms.

Intramolecular hydrogen bonds are considered to be most significant interactions for the stability of a protein structure [44]. Thus we examined the trajectory file for fluctuations in H bond frequencies of native and mutant (G820S and G856S) Axin1 protein models with respect to time in order to analyze the relationship between flexibility and NH bond formation (Fig. 3). The native Axin1 structure exhibited an average ~125 to ~165 hydrogen bonds throughout the simulation period. Mutant structure G820S showed variation in H bonds ranging from ~122 to ~163, on the other side mutant model G856S exhibited variations in H bonds ranging from ~125 to ~166. During the simulation analysis the results clearly depict a real time image of variations in the H bond frequencies in the mutant Axin1 models compared to native. This fluctuation in H bond frequencies of mutant models from the native Axin1 protein depicts the deleterious impact of these single nucleotide polymorphisms on the 3D structure of the Axin1 protein. These fluctuations in the H bond frequencies justify the variation in the RMSF and Rg values, since atomic flexibilities are mostly dependent on the H bonds formed by them in the protein structure.

The surface of protein in contact with the surrounding solvent is denoted as the solvent accessible surface area (SASA). Protein stability and rearrangement of the protein residues during protein folding are mainly determined by the solvation process of the protein. Thus SASA values of the native and mutant models were analyzed in Fig. 3. Native Axin1 structure showed SAS values ranging from ~80–88 nm^2, whereas the mutant model G820S showed slight variation in SAS values from ~75–84 nm^2. On the other side, significant variations were noted for the mutant model having SAS values ranging from 72–82 nm^2.

Molecular Docking

Protein-protein interactions are known to play prominent role in various cellular processes which are also implicated in various diseases and thus, are a high value target for therapeutic interventions [45]. Hereby, considering the importance of Axin1 protein in Wnt pathway destruction complex, we studied the interaction of native and mutant Axin1 protein structures and the proteins involved in the destruction complex (APC and GSK3β). The 3D structures of APC and GSK3β were obtained from Uniprot having PDB ids-3NMZ and 3DU8, respectively. Hex docking results provided the total binding energies of all the six protein–protein dock complexes. Results illustrated variation in total binding energies of wild Axin1 protein and mutant Axin1 models with destruction complex proteins shown in Table 6. Binding energies of wild Axin1protein with APC protein showed value of −552.5 KJ/mol, whereas mutant models G820S and G856S showed values of −570.7 and −570.7 KJ/mol, respectively. Higher variations in binding energies were observed during interaction of models G820S and G856S with GSK3β proteins. Wild Axin1 interaction with GSK3β showed binding energy values of −656.5 KJ/mol. On the other side, the mutant models G820S and G856S interactions with GSK3β showed binding energy values of −802.4 and −498.8 KJ/mol, respectively (Fig. 4). Further, the ZDOCK results followed the similar pattern in the docking scores, showed in Table 7. ZDOCK score of wild Axin1protein with APC protein showed value of 1489.934, whereas mutant models G820S and G856S showed values of 1534.362 and 1534.362 respectively. Similarly, higher variations in ZDOCK score were observed from interaction of models G820S and G856S with GSK3β proteins. Wild Axin1 interaction with GSK3β showed ZDOCK score values of 1570.634. On the other side the mutant models G820S and G856S interactions with GSK3β showed binding energy values of 1589.371 and 1539.374. These results further strengthen our theory, that these (G820S and G856S) single nucleotide polymorphism causes deleterious effects on the structural and functional attributes of the Axin1 protein.

Discussion

Axin 1 is a scaffold protein with multiple domain for interacting with several different proteins of Wnt signaling pathway [46]. Axin1 has been demonstrated as a tumor suppressor gene and found to play crucial role in human CRC [47]. Several gene mutations have been identified through out the Axin 1 gene sequence and found to be associated with different cancers [66]. Thus, Axin 1 can be a possible molecular target for developing diagnostic and therapeutic strategies. Accordingly, aim of this study was to prioritize deleterious single nucleotide polymorphisms and their damaging effect on the structural and functional attributes of Axin 1 protein (Table 8).

A disease associated gene variant exhibits complex association with patients genetic background, stochastic influences and environmental factors;the clinical expression of the mutation is also an important variable among different individuals [48]. These limitations in investigating the genotype–phenotype correlation and their association with disease status make it highly challenging and costly [49]. To overcome these challenges, recent advances in bioinformatics approaches to study single nucleotide

Table 6 Hex total energy values (KJ/mol) for native and mutant Axin1 structures with destruction complex proteins

Sl. No.	Docked structures	Binding energy
1	WILD-GSK3β	−656.5
2	Mutant 820-GSK3β	−802.4
3	Mutant 856-GSK3β	−498.8
4	WILD-APC	−552.5
5	Mutant 820-APC	−570.7
6	Mutant 856-APC	−570.7

Table 7 Z Dock scores for native and mutant Axin1 structures with destruction complex proteins

Docked molecules	Z Dock score
WILD-GSK3β	1570.634
Mutant 820-GSK3β	1589.371
Mutant 856-GSK3β	1539.374
WILD-APC	1489.934
Mutant 820-APC	1534.362
Mutant 856-APC	1534.362

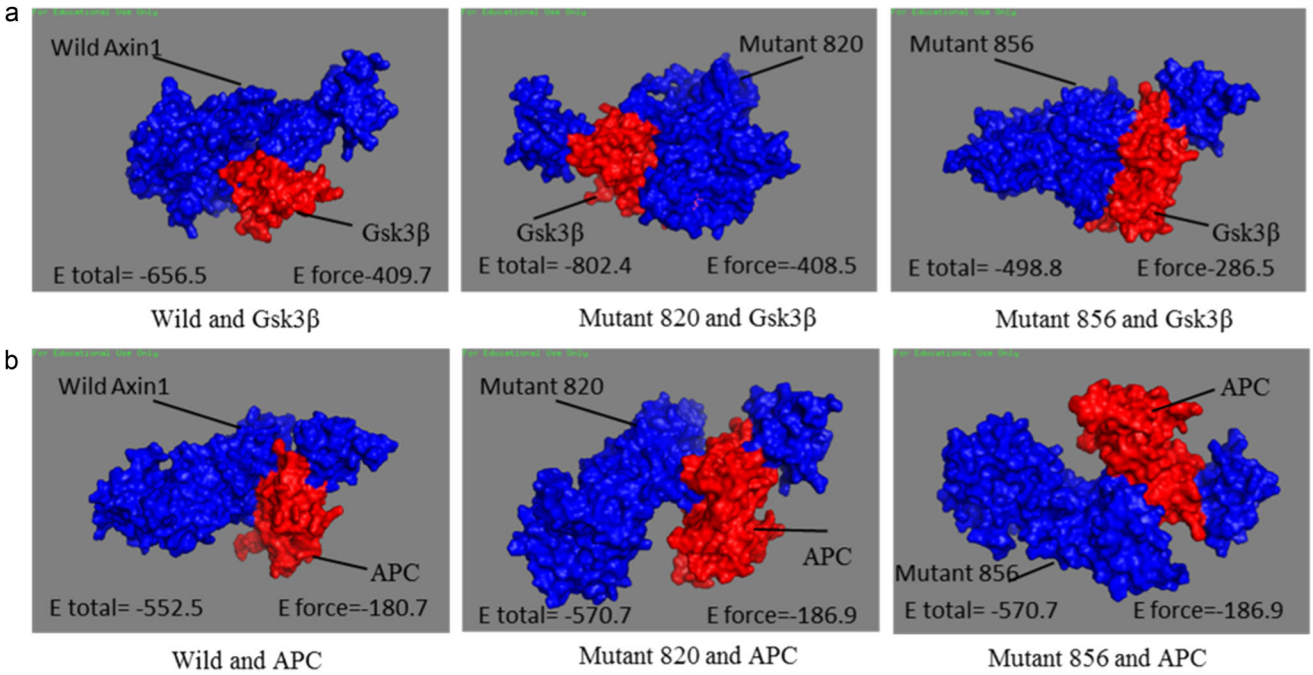

Fig. 4 Computational model of native and mutant (G820S and G856S) models docked to **a** GSK3β and **b**. APC

polymorphisms and amino acid residue changes have progressively gained attention of researchers [50].To the best our knowledge, thisstudy provides first demonstration of functionally deleterious SNPs associated with the Axin1 gene through in silico approach.

In the present study, we attempted to evaluate and prioritize the deleterious nsSNPs of Axin1 gene in four contexts: (1) Identification of deleterious nsSNP by both sequence based and structure based approaches (PROVEAN, PolyPhen-2, and I-Mutant 2.0), (2) Investigation of the changes in various structural attributes (Secondary structures, Solvent accessibility, Flexible residues and Intramolecular hydrogen bond), (3) Analysis of the 3D structures by molecular dynamics simulation, (4) Evaluation of the deleterious effect of nsSNPs over the interactions of Axin1 protein with destruction complex proteins through Hex and ZDOCK protein-protein docking tool. To achieve this, we extracted the SNP data for Axin1 gene from NCBI database and nsSNPs were sorted for further in silico analysis through different computational tools. A number of recent researches have documented that implementing multiple bioinformatics tools and algorithms enhance the accuracy of the results [51–53]. Thus, we employed different tools like PROVEAN, Polyphen-2, and I-Mutant-2.0 predicts the phenotypic effect of the nsSNPs on the basis of protein sequence conservation and protein structure [20–24]. To minimize any possible false positive results, we further incorporated cumulative approach by comparing and combining the results of all the three tools. Thus, we selected 6 nsSNPs which were predicted to be deleterious by all the three tools (Table 1).

It is crucial to gain better understanding of functional impact of a single nucleotide substitution in a gene sequence without gaining information about the 3D structure of the protein encoded by the gene. So, multiple 3D structures of Axin1 protein, to complete the trajectory analysis, were obtained from Universal Protein Resource (UniProt), followed by the validation of the native structure

Table 8 Native and mutant Axin 1 protein sequence denoting the amino acid substitutions

Sl. No.	Residue change	Amino acid sequences
1	Native	MNIQEQGFPLDLGASFTEDAPRPPVPGEEGELVSTDPRPASYSFCSGKGVGIKGETSTATPRRSDL DLGYEPEGSASPTPPYLKWAESLHSLLDDQDGISLFRTFLKQEGCADLLDFWFACTGFRKLEPCD SNEEKRLKLARAIYRKYILDNNGIVSRQTKPATKSFIKGCIMKQLIDPAMFDQAQTEIQATMEEN TYPSFLKSDIYLEYTRTGSESPKVCSDQSSGSGTGKGISGYLPTLNEDEEWKCDQDMDEDDGRDA APPGRLPQKLLLETAAPRVSSSRRYSEGREFRYGSWREPVNPYYVNAGYALAPATSANDSEQQS LSSDADTLSLTDSSVDGIPPYRIRKQHRREMQESVQVNGRVPLPHIPRTYRVPKEVRVEPQKFAE ELIHRLEAVQRTREAEEKLEERLKRVRMEEEGEDGDPSSGPPGPCHKLPPAPAWHHFPPRCVDM GCAGLRDAHEENPESILDEHVQRVLRTPGRQSPGPGHRSPDSGHVAKMPVALGGAASGHGKHV PKSGAKLDAAGLHHHRHVHHHVHHSTARPKEQVEAEATRRAQSSFAWGLEPHSHGARSRGYS ESVGAAPNASDGLAHSGKVGVACKRNAKKAESGKSASTEVPGASEDAEKNQKIMQWIIEGEKEI SRHRRTGHGSSGTRKPQPHENSRPLSLEHPWAGPQLRTSVQPSHLFIQDPTMPPHPAPNPLTQLEE ARRRLEEEEKRASRAPSKQRTRSQRKVGGGSAQPCDSIVVAYYFCGEPIPYRTLVRGRAVTLGQ FKELLTKKGSYRYYFKKVSDEFDCGVVFEEVREDEAVLPVFEEKII**G**KVEKVDRYYFKKVSDEF DCGVVFEEVREDEAVLPVFEEKII***G***KVEKVD

Note: Highlighted amino acid residue denotes the point of substitution and the respective positions, bold: denotes G820S and bold italic: denotes G856S

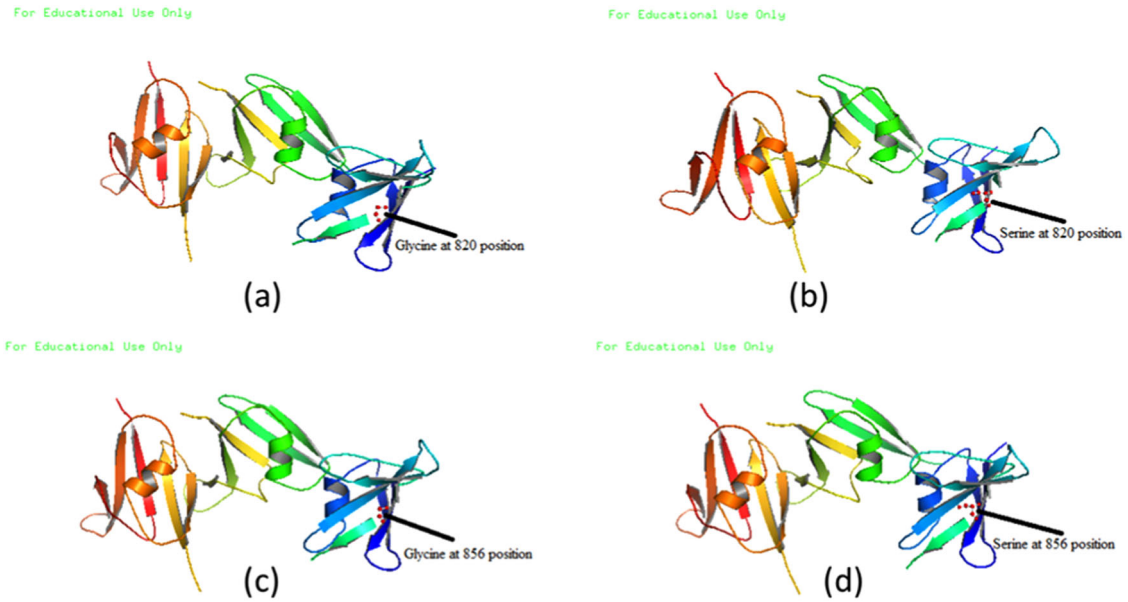

Fig. 5 3D structures of native and mutant Axin 1 protein; **a** Native protein denoting glycine at 820 position, **b** Mutant protein denoting serine at 820 position, **c** Native protein denoting glycine at 856 position and **d** Mutant protein denoting serine at 856 position

by using PROCHECK server. The structure had resolution of 1.57, 2.40, and 2.90 A° and Ramachandran plot depicted the presence of higher number of residues in most favored region. Mutant models for the 6 highly deleterious nsSNPs sorted through combinatorial analysis were generated by using SWISSPDB Viewer. Further analysis on mutant Axin1 models was performed after the energy minimization of the three dimensional structures using NOMAD-Ref server. It is well established that stability to protein structures are provided via various non-covalent interactions, e.g., hydrophobic, Vander waals, non-covalent, and electrostatic interactions [54, 55]. Hydrophobic interactions are thought to be the driving forces for the protein folding [56]. Similarly, the tendency to resist the folding is derived from cooperative interactions between residues in protein structure [57, 58]. For further deep understanding of deviation in the mutant Axin1 structure due to single nucleotide polymorphisms, we performed trajectory analysis to find the insight of the structural deviation in the protein structure. The trajectory analysis involved the identification of the stabilizing residues, hydrogen bond frequencies, flexible residues, solvent accessibility, and secondary structures prediction of selected mutant Axin1 models having highly deleterious nsSNPs. Thereafter, by comparing and combining the results of SRide and SPPIDER tools, we selected 2 nsSNPs (G820S and G856S) that were predicted to have

variation in stabilizing residues and solvent accessibility from native Axin1 protein model. Therefore, we further analyzed the hydrogen bond frequencies and flexible residues in G820S and G856S mutant models and compared with the native Axin1 protein model. The results showed notable difference in number of flexible residues and intramolecular hydrogen bond frequencies. The investigation of different structural attributes clearly depicted the deleterious impact of single nucleotide substitution in gene sequence of Axin1, causing the amino acid residue change in Axin1 proteinwhich could be damaging to the structural integrity of Axin 1 protein. 3D structure of native and mutant Axin 1 protein were drawn via PyMol molecular graphics system depicting a clear image of the residue changes in Fig. 5 [59].

To further strengthen the analysis of G820S and G856S mutant models, we employed the real-time 3D molecular dynamics simulation approach. MD analysis of both mutant models in comparison to native Axin1 protein structure adds an extra dimension to the investigation. The results of MD provided the RMSD, RMSF, Rg, Number of hydrogen bond, and SASA values. The degree of fluctuation in the 3D structures is established by analyzing RMSD and Rg value over time. Results showed that the changes in geometry of atom in both the mutant models varied over time during the simulation. This highlights the decrease in stability of the mutant models. Findings of the MD analysis for number of hydrogen bonds and SASA values were in concordance to the results of trajectory analysis. Thus, the deleterious impact of both nsSNPs G820S and G856S was well established through a systematic analysis of various sequence and structural aspects of Axin1 protein.

Protein–protein interactions are critical for the cellular signaling pathways and deleterious nsSNPs causing phenotypic changes in the proteins can lead to deregulated signaling pathways. Axin 1 play very important role in the assembly of destruction complex members which is crucial for the regulation of Wnt/ β-catenin pathway. GSK3β has been shown to fecilitate the phosphorylation of β-catenin in cooperation with APC and Axin1 and its subsequent degradation by proteasome complex [60]. Moreover, deletion/overexpression of APC and inhibition of GSK3β have been correlated with CRC development [61, 62]. Thus, functional impact of G820S and G856S nsSNPs on the interaction of Axin1 protein with the Wnt pathway destruction complex members, APC and GSK3β was assessed by hex 5.1 molecular docking tool and ZDOCK. The binding energies of native and mutant Axin1 protein models with APC and GSK3β proteins showed notable differences. According to previous studies, the hex binding energy and ZDOCK score denote the binding affinity between interacting molecules [63–65]. Therefore, the variation in the Hex total binding energies and ZDOCK scores reflect the change in interaction of native and mutant Axin1 and destruction complex protein APC and GSK3β. Since the interaction between destruction complex proteins Axin1, APC, and GSK3β play very crucial role in Wnt signaling pathway, slight variations in the structural and functional attributes are of great importance to be considered. Thus, in summary the results of our present study suggested two highly deleterious nsSNPs G820S and G856S of Axin1 gene that can be further undertaken for epidermiological studies to analyze the phenotypic association and correlation in human CRC.

Conclusion

In conclusion, this study attempts to prioritize highly deleterious missense mutations in coding region of Axin1 gene. Through systematic combinatorial in silico investigation of Axin1 gene having 100 nsSNPs in coding region, led to prioritizing two highly deleterious missense mutations G820S and G856S recognized as rs142888154. Furthermore, structural and functional analysis through molecular dynamics and molecular docking predicted the possible deleterious effect of these SNPs on Axin1 protein. Although insight on pathological activities and outcomes of these SNPs has not been gained, but the results strongly suggest that they can play crucial role in the structural and functional aspects of Axin1 protein. Since, the methods involved in determining the structural and functional impact of each and every SNP are difficult, expensive and time consuming for a researcher. Thus, the study paves a way to prioritize and predict the highly deleterious nsSNPs of Axin1 gene in a less time consuming and cost effective manner and could be an adjunt in the disease genotype phenotype correlation studies.

Acknowledgements The authors thank the management of the Integral University for providing the facilities to carry out this study and also greatly thankful to Maulana Azad National Fellowship (MANF), University gratns Commission (UGC), Government of India, for providing senior research fellowship (SRF) to IK.

Compliance with ethical standards

Conflict of interest The authors declare that they have no competing interests.

References

1. Roy, S., & Majumdar, A. P. N. (2012). Signaling in colon cancer stem cells. *Journal of Molecular Signaling*, *7*, 11.
2. Brabletz, S., Schmalhofer, O., & Brabletz, T. (2009). Gastrointestinal stem cells in development and cancer. *Jounal of Pathology*, *217*, 307–317.

3. Korkaya, H., Paulson, A., Charafe-Jauffret, E., Ginestier, C., Brown, M., Dutcher, J., Clouthier, S. G., & Wicha, M. S. (2009). Regulation of mammary stem/progenitor cells by PTEN/Akt/beta-catenin signaling. *PLoS Biology*, *7*, e1000121.
4. He, X. C., Zhang, J., Tong, W. G., Tawfik, O., Ross, J., Scoville, D. H., Tian, Q., Zeng, X., He, X., Wiedemann, L. M., Mishina, Y., & Li, L. (2004). BMP signaling inhibits intestinal stem cell self-renewal through suppression of Wnt–β-catenin signaling. *Nature Genetics*, *36*, 1117–1121.
5. Zeng, L., Fagotto, F., Zhang, T., Hsu, W., Vasicek, T. J., Perry, W. L., Lee, J. J., Tilghman, S. M., Gumbiner, B. M., & Costantini, F. (1997). The mouse Fused locus encodes Axin, an inhibitor of the Wnt signaling pathway that regulates embryonic axis formation. *Cell*, *90*, 181–192.
6. Hsu, W., Zeng, L., & Costantini, F. (1999). Identification of a domain of Axin that binds to the serine/threonine protein phosphatase 2A and a self-binding domain. *Journal of Biological Chemistry*, *274*, 3439–3445.
7. Kishida, S., Yamamoto, H., Hino, S., Ikeda, S., Kishida, M., & Kikuchi, A. (1999). DIX domains of Dvl and axin are necessary for protein interactions and their ability to regulate β-catenin stability. *Molecullar and Cellular Biology.*, *19*, 4414–4422.
8. Hart, M. J., de los Santos, R., Albert, I. N., Rubinfeld, B., & Polakis, P. (1998). Downregulation of -catenin by human Axin and its association with the APC tumor suppressor, -catenin and GSK3. *Current Biology.*, *8*, 573–581.
9. Hinoi, T., Yamamoto, H., Kishida, M., Takada, S., Kishida, S., & Kikuchi, A. (2000). Complex formation of adenomatous polyposis coli gene product and axin facilitates glycogen synthase kinase-3-dependent phosphorylation of -catenin and downregulates–catenin. *Journal of Biological Chemistry*, *275*, 34399–34406.
10. Aberle, H., Bauer, A., Stappert, J., Kispert, A., & Kemler, R. (1997). β-catenin is a target for the ubiquitin-proteasome pathway. *EMBO Journal*, *16*, 3797–3804.
11. Fagotto, F., Jho, E., Zeng, L., Kurth, T., Joos, T., Kaufmann, C., & Costantini, F. (1999). Domains of axin involved in protein-protein interactions, Wnt pathway inhibition, and intracellular localization. *Journal of Cellular Biology*, *145*, 741–756.
12. Kishida, S., Yamamoto, H., Hino, S., Ikeda, S., Kishida, M., & Kikuchi, A. (1999). DIX domains of Dvl and axin are necessary for protein interactions and their ability to regulate -catenin stability. *Molecular and Cellular Biology*, *19*, 4414–4422.
13. Sakanaka, C., & Williams, L. T. (1999). Functional domains of axin. Importance of the C terminus as an oligomerization domain. *Journal of Biological Chemistry*, *274*, 14090–14093.
14. Burgess, A. W., Faux, M. C., Layton, M. J., & Ramsay, R. G. (2011). Wnt signaling and colon tumorigenesis--a view from the periphery. *Experimental Cell Research.*, *317*, 2748–2758.
15. Bienz, M., & Clevers, H. (2000). Linking colorectal cancer to Wnt signaling. *Cell*, *103*, 311–320.
16. Miller, J. R., Hocking, A. M., Brown, J. D., & Moon, R. T. (1999). Mechanism and function of signal transduction by the Wnt/-catenin and Wnt/Ca2pathways. *Oncogene*, *18*, 7860–7872.
17. Smalley, M. J., & Dale, T. C. (1999). Wnt signalling in mammalian development and cancer. *Cancer Metastasis Reviews*, *18*, 215–230.
18. Vogelstein, B., Fearon, E. R., Hamilton, S. R., Kern, S. E., Preisinger, A. C., Leppert, M., Nakamura, Y., White, R., Smits, A. M., & Bos, J. L. (1998). Genetic alterations during colorectal-tumor development. *The New England. Journal of Medicine*, *319*, 525–532.
19. Lustig, B., & Behrens, J. (2003). the Wnt signaling pathway and its role in tumor development. *Journal of Cancer Resources Clinical Oncology*, *129*, 199–221.
20. Burke, D. F., Worth, C. L., Priego, E., Cheng, T., Smink, L. J., Todd, J. A., & Blundell, T. L. (2007). Genome bioinformatic analysis of nonsynonymous SNPs. *BMC Bioinformatics*, *8*, 301–315.
21. Chasman, D., & Adams, R. M. (2001). Predicting the functional consequences of nonsynonymous single nucleotide polymorphisms: Structure-based assessment of amino acid variation. *Journal of Molecular Biology*, *307*, 683–706.
22. Sunyaev, S., Ramensky, V., Koch, I., Lathe, W., Kondrashov, A., & Bork, P. (2001). Prediction of deleterious human alleles. *Human Molecule Genetics*, *10*, 591–597.
23. Wang, Z., & Moult, J. (2001). SNPs, protein structure, and disease. *Human Mutation*, *17*, 263–270.
24. Grantham, R. (1974). Amino acid difference formula to help explain protein evolution. *Science*, *185*, 862–864.
25. Rajith, B., & George, P. D. C. (2011). Path to facilitate the prediction of functional amino acid substitutions in red blood cell disorders–A computational approach. *PLoS ONE*, *6*, e24607.
26. Sherry, S. T., Ward, M. H., Kholodov, M., Baker, J., Phan, L., Smigielski, E. M., & Sirotkin, K. (2001). dbSNP: The NCBI database of genetic variation. *Nucleic Acids Research*, *29*, 308–311.
27. Choi, Y., Sims, G. E., Murphy, S., Miller, J. R., & Chan, A. P. (2012). Predicting the functional effect of amino acid substitutions and indels. *PLoS ONE*, *7*, e46688.
28. Ramensky, V., Bork, P., & Sunyaev, S. (2002). Human non-synonymous SNPs: server and survey. *Nucleic Acids Research*, *30*, 3894–3900.
29. Adzhubei, I. A., Schmidt, S., Peshkin, L., Ramensky, V. E., Gerasimova, A., & Bork, P. (2010). A method and server for predicting damaging missense mutations. *Nature Methods*, *7*, 248–249.
30. Bava, K. A., Gromiha, M. M., Uedaira, H., Kitajima, K., & Sarai, A. (2004). ProTherm, version 4.0: thermodynamic database for proteins and mutants. *Nucleic Acids Resorces*, *32*, D120–D121.
31. Laskowski, R. A., Rullmannn, J. A., MacArthur, M. W., Kaptein, R., & Thornton, J. M. (1996). AQUA and PROCHECK-NMR: programs for checking the quality of protein structures solved by NMR. *Journal of Biomolecular NMR*, *8*, 477–486.
32. Laskowski, R. A., MacArthur, M. W., & Thornton, J. M. (2001). *PROCHECK: validation of protein structure coordinates, in international tables of crystallography, Volume F. crystallography of biological macromolecules.* In M. G. Rossmann & E. Arnold (eds.), *Dordrecht* (pp. 722–725). The Netherlands: Kluwer Academic Publishers.
33. Lindahl, E., Azuara, C., Koehl, P., & Delarue, M. (2006). NOMAD-Ref: visualization, deformation and refinement of macromolecular structures based on all-atom normal mode analysis. *Nucleic Acids Res*, *34*, W52–56.
34. Porollo, A., & Meller, J. (2007). Prediction-based fingerprints of protein-protein interactions. *Proteins Structure Function and Bioinformatics*, *66*, 630–645.
35. Magyar, M., Gromiha, M. M., Pujadas, G., Tusnady, G. E., & Simon, I. (2005). SRide: a server for identifying stabilizing residues in proteins. *Nucleic Acids Res*, *33*, W303–W305.
36. Kuznetsov, I. B. (2008). Ordered conformational change in the protein backbone: prediction of conformationally variable positions from sequence and low-resolution structural data. *Proteins: structure, Functinal Bioinfo*, *72*, 74–87.
37. Tiwari, A., & Panigrahi, S. K. (2007). HBAT: A complete package for analysing strong and weak hydrogen bonds in macromolecular crystal structures. *In Silico Biology*, *7*, 651–661.
38. Hess, B., Kutzner, D., & Spoel, D. (2008). GROMACS 4:Algorithms for highly efficient, load-balanced, and scalable molecular

simulation. *Journal of Chemical Theory and Computation*, *4*, 435–447.
39. Raghuraman, P., Sudan, R.J.J., Kumari, J.L.J., Sudandiradoss, C. (2016). Casting the critical regions in Nucleotide binding oligomerization domain 2 protein: A signature mediated structural dynamics approach, *Journal of Biomolecular Structure and Dynamics*, doi:10.1080/07391102.2016.1254116.
40. Ritchie, D. W., & Kemp, G. J. L. (2000). Protein Docking Using Spherical Polar Fourier Correlations. *Proteins*, *39*, 178–194.
41. Chen, R., & Weng, Z. (2002). Docking unbound proteins using shape complementarity, desolvation, and electrostatics. *Proteins*, *47*, 281–294.
42. Yuan, H. Y., Chiou, J. J., Tseng, W. H., Liu, C. H., Liu, C. K., Lin, Y. J., Wang, H. H., Yao, A., Chen, Y. T., & Hsu, C. N. (2006). FASTSNP: an always up-to-date and extendable service for SNP function analysis and prioritization. *Nucleic Acids Resources*, *34*, 635–41.
43. Grillo, G., Turi, A., Licciulli, F., Mignone, F., Liuni, S., Banfi, S., Gennarino, V. A., Horner, D. S., Pavesi, G., Picardi, E., & Pesole, G. (2010). UTRdb and UTRsite (RELEASE 2010) a collection of sequences and regulatory motifs of the untranslated regions of eukaryotic mRNAs. *Nucleic Acids Resources*, *38*, D75–80.
44. Eisenberg, D., & McClachlan, A. (1986). Solvation energy in protein folding and binding. *Nature*, *319*, 199–203.
45. Berg, T., Cohen, S. B., Desharnais, J., Sonderegger, C., Maslyar, D. J., Goldberg, J., Boger, D. L., & Vogt, P. K. (2002). Small-molecule antagonists of MycMax dimerization inhibit Myc-induced transformation of chicken embryo fibroblasts. *PNAS*, *99*, 63830–3835.
46. Zeng, L., Fagotto, F., Zhang, T., Hsu, W., Vasicek, T. J., Perry, W. L., Lee, J. J., Tilghman, S. M., Gumbiner, B. M., & Costantini, F. (1997). The mouse Fused locus encodes Axin, an inhibitor of the Wnt signaling pathway that regulates embryonic axis formation. *Cell*, *90*, 181–192.
47. Satoh, S., Daigo, Y., Furukawa, Y., Kato, T., Miwa, N., Nishiwaki, T., Kawasoe, T., Ishiguro, H., Fujita, M., Tokino, T., Sasaki, Y., Imaoka, S., Murata, M., Shimano, T., Yamaoka, Y., & Nakamura, Y. (2000). AXIN1 mutations in hepatocellular carcinomas, and growth suppression in cancer cells by virus-mediated transfer of AXIN1. *Nature Genetics*, *24*, 245–250.
48. Watkins, H. (2001). Hypertrophic cardiomyopathy: From molecular and genetic mechanisms to clinical management. *European Heart Journal*, *3*, L43–L50.
49. Kumar, A., Rajendran, V., Sethumadhavan, R., Shikla, P., Tiwari, S., & Purohit, R. (2014). Computational SNP Analysis: Current approaches and future prospects. *Cell Biochemical Biophysics*, *68*, 233–239.
50. Frederic, M. Y., Lalande, M., Boileau, C., Hamroun, D., Claustres, M., Beroud, C., & Collod-Beroud, G. (2009). UMD-predictor, a new prediction tool for nucleotide substitution pathogenicity - application to four genes: FBN1, FBN2, TGFBR1, and TGFBR2. *Human Mutation*, *30*, 952–959.
51. Khan, I., Ansari, I. A., & Singh, P. (2016). Prediction of functionally significant single nucleotide polymorphisms [SNPs] in PTEN tumor suppressor gene: An in silico approach, *Biotechnology Application of Biochemical*. doi:10.1002/bab.1483.
52. Ramesh, A. S., Khan, I., Farhan, M., & Thiagarajan, P. (2013). Profiling Deleterious Non-Synonymous SNPs of CYP1A1 Gene in Smokers. *Cell Biochemistry and Biophysics*, *67*, 1391–1396.
53. Ramesh, A. S., Sethumadhavan, R., & Thiagarajan, P. (2013). Structure–Function Studies on Non-synonymous SNPs of Chemokine Receptor Gene Implicated in Cardiovascular Disease: A Computational Approach. *Protein Journal*, *32*, 657–665.
54. Han, J. H., Kerrison, N., Chothia, C., & Teichmann, S. A. (2006). Divergence of interdomain geometry in two-domain proteins. *Structure*, *14*, 935–945.
55. Dill, K. A. (1990). Dominant forces in protein folding. *Biochemistry*, *29*, 7133–7155.
56. Ponnuswamy, P. K., & Gromiha, M. M. (1994). On the conformational stability of folded proteins. *Journal of Theorical. Biology*, *166*, 63–74.
57. Ponnuswamy, P. K. (1993). Hydrophobic characteristics of folded proteins. *Program Biophysics Molecular Biological*, *59*, 57–103.
58. Abkevich, V. I., Gutin, A. M., & Shakhnovich, E. I. (1995). Impact of local and non-local interactions on thermodynamics and kinetics of protein folding. *Journal of Molecular Biological*, *252*, 460–471.
59. DeLano, W. L. (2010). The PyMOL molecular graphics system, Version 1.3r1. South San Carlos, CA: DeLano Scientific LLC.
60. Metcalfe, C., & Bienz, M. (2011). Inhibition of GSK3 by Wnt signalling–two contrasting models. *Journal of Cell Science*, *124*, 3537–3544.
61. Merritt, A. J., Gould, K. A., & Dove, K. A. W. F. (1997). Polyclonal structure of intestinal adenomas in ApcMin/+mice with concomitant loss of Apc^{+} from all tumor lineages. *Proceedings of the Natlional Academic Science USA*, *94*, 13927–13931.
62. Novelli, M. R., Williamson, J. A., Tomlinson, I. P., Elia, G., Hodgson, S. V., Talbot, I. C., Bodmer, W. F., & Wright, N. A. (1996). Polyclonal origin of colonic adenomas in an XO/XY patient with FAP. *Science*, *272*, 1187–1190.
63. Babahedari, A. K., Shamsabadi, M. K., kabiri, H. R., & Tavakoli, Kh (2013). Docking studies of competitive interaction of human serum albumin with ibuprofen an d aspirin using the HEX docking software. *Journal of Emerging Trends in Computing and Information Sciences*, *4*, 97–99.
64. kumar, R., Sanjuktha, M., Singarave, R., Ramakrishnan, S., Rajan, J. J. S., kumar Sl, S. S., Poornima, M., Santiago, T. C., & Alavandi, S. V. (2012). Molecular modelling and docking studies on shrimp vitellogenin receptor and ligand target mediated delivery system. *International Journal of Research in Drug Delivery*, *2*, 11–14.
65. Prakash, N., Patel, S., Faldu, N. J., Ranjan, R., & Sudhe, D. V. N. (2010). Molecular docking studies of antimalarial drugs for malaria. *Journal Computation Sciences System Biology*, *3*, 070–073.